

Reactive Compatibilization of PLA/TPU Blends with a Diisocyanate

Sebnem Kemaloglu Dogan,¹ Efren Andablo Reyes,² Sanjay Rastogi,² Guralp Ozkoc¹

¹Department of Chemical Engineering, Kocaeli University, 41380, Kocaeli, Turkey

²Department of Materials, Loughborough University, Loughborough, Leicestershire LE11 3TU, United Kingdom

Correspondence to: G. Ozkoc (E-mail: guralp.ozkoc@kocaeli.edu.tr)

ABSTRACT: This study focuses on the compatibilization of poly(lactic acid) (PLA)/thermoplastic polyurethane (TPU) blends by using 1,4 phenylene diisocyanate (PDI) for the first time, as the compatibilizer. Because of the potential interactions of diisocyanates with —OH/—COOH, they are useful for reactive processing of PLA/TPU blends in the melt processing. To have insight on the reactively compatibilized structure of PLA/TPU blends, phase morphologies are observed by means of scanning electron microscopy. The mechanical, thermal, and rheological responses of the blends are investigated. The observations are that the brittle behavior of PLA changes to ductile with the addition of TPUs. The addition of PDI improves the tensile properties of the blends. The compatibilization action of PDI is monitored with DMA and rheological experiments. Cross-over in the G' and G'' curves of compatibilized blends indicates the relaxation of branches formed in the presence of PDI. The dispersed phase size of TPU decreases in PLA in the presence of PDI due to the improved compatibility. © 2013 Wiley Periodicals, Inc. *J. Appl. Polym. Sci.* **2014**, *131*, 40251.

KEYWORDS: polylactide; blends; biodegradable; rheology; mechanical properties

Received 8 November 2013; accepted 3 December 2013

DOI: 10.1002/app.40251

INTRODUCTION

The increasing use of petrochemical based nondegradable polymers negatively affects the ecology due to the huge accumulation of solid wastes disposed to environment. In addition, the incineration of these wastes increases the CO₂ emission and subsequently contributes to global warming. One of the sustainable solutions of this problem is the use of biodegradable and biocompatible polymers. Recently, poly(lactic acid) (PLA) has attracted attention because of its industrial scale production with a comparable price to other petroleum-based polymers. PLA is synthetic biodegradable aliphatic polyester derived from renewable sources such as wheat, corn, potato, sugarcane, etc. PLA is mainly synthesized by ring opening polymerization of lactide, which is the cyclic dimer of lactic acid.¹ Although PLA is relatively high strength and high modulus analogous to polystyrene, its inherent brittleness and low toughness due to the low entanglement density and the high value of characteristic ratio representing the chain stiffness restrict its application.^{1–3}

In comparison to other methods, such as copolymerization of lactide with other monomers^{4,5} and plasticization with low molecular weight miscible compounds,^{6,7} blending of PLA with high molecular weight flexible polymers is a more practical and economical way of toughening of the polymer.^{8,9} However, most of the polymer blends exhibit multiphase morphology due to the immiscible character of the components and as a

consequence, this limits blends' performance due to low interfacial adhesion. In order to overcome this problem, compatibilization is required.¹⁰ Reactive processing is a commonly used compatibilization method to obtain cost-effective production of new polymeric blends with enhanced performance. In reactive compatibilization, terminal or graft groups of the compatibilizers react with the terminal group of the both components of the blend yielding block or graft copolymers during melt processing.

Recently, a number of studies have been published on the compatibilization of PLA-based blends.^{11–16} Among these studies, Shin and Han utilized glycidyl methacrylate (GMA) in combination with electron beam radiation for successful compatibilization of PLA/poly(ϵ -caprolactone) blends.¹¹ Wootthikanokkhan et al. synthesized PLA-graft-maleated thermoplastic starch and investigated the compatibilization efficiency in the blends.¹² Lee and Kim investigated the potential usage of PP-g-MAH and PE-g-GMA individually or together to make tough PP/PLA blends (Biomax[®] Strong 120).¹³ Wang et al. studied thermal and mechanical properties, and morphology of modified PLA/polycarbonate (PC) blends in the presence of poly(butylene succinate-co-lactate) (PBSL) and epoxy as the compatibilizers.¹⁴ Takayama et al. prepared PLA/PCL blend with lysine triisocyanate as compatibilizer to improve compatibility of components.¹⁵ Kumar et al. introduced reactive processing agent GMA as a plasticizer to improve the interphase balance between the PLA/

poly(butylene adipate-*co*-terephthalate) (PBAT) blends.¹⁶ From the reported studies, it is apparent that to improve the properties of PLA-based immiscible blends a compatibilizer is required.

Thermoplastic polyurethanes (TPUs) are a well-known family of polymers having good mechanical properties balanced with biocompatibility, biostability,^{17–21} and biodegradability.^{17,22} TPUs are segmented copolymers consisting of alternating hard segment formed from a diisocyanate and a chain extender, and the soft segment is mainly derived from a polyester or polyether-based polyol. It is possible to tune properties of a TPU by changing the hard to soft segment ratio and their respective chemistry to fulfill the requirements of the intended applications.²³ Besides the relatively lower melting temperature and higher decomposition temperature, TPUs provide a wide processing window. TPUs can also be used to toughen the PLA^{20,24–27} because the soft segment of a TPU is mainly polyester or polyether, which is expected to have good compatibility with PLA. In addition, similar to PLA, most of the TPUs are FDA-approved polymers^{27,28} that confirms the biodegradability and biocompatibility requirements of PLA-based blends. The isocyanate component of TPUs is still considered toxic if it is inhaled or exposed.²⁹ On the other hand, because of the high reactivity of isocyanates, it has been assumed that no residual isocyanate will remain in the end products.³⁰

Han and Huang recently investigated the properties of PLA/TPU blends.²⁴ They found that blending of TPU improves the toughness of the PLA as observed from Izod impact tests and tensile tests. The morphological analysis indicated that the size of the spherical TPU particles, uniformly dispersed in the PLA matrix, decreases with the increasing TPU content. Feng and Ye studied the properties of PLA/TPU blends, having different blending composition, to explore a potential method for improving the toughness of PLA.³¹ The results conclusively showed that with the addition of TPU brittle PLA changes into ductile apparent from the deformation via neck formation. The authors mentioned that the blends were partially miscible because of the hydrogen bonding between the molecules of PLA and TPU though the homogeneous dispersion of TPU particles in PLA matrix was obtained. Micromechanical characterization, to judge the toughness of the blends, showed that the toughened blends had increased crack initiation resistance and crack propagation resistance. Similar to the study by Feng and Ye, Li and Shimuzi examined the toughness based properties of PLA/poly(ether)urethane blends.²⁰ The shifts in T_g values of PLA and TPU phases, obtained from DMA analysis, in the blends lead to the conclusion that the two polymers were partially miscible. It was mentioned that the addition of PU elastomer not only accelerated the crystallization speed but also decreased crystallinity of the PLA. In addition, with an increase of the TPU content, the blend showed increase in elongation and impact strength indicating toughening of the TPU elastomer on the PLA. In another study, Hong et al. examined the miscibility of PLA/TPU blends at varying compositions.³² They found that the blend was partially miscible with shift in glass transition temperature.

From the available literature, it is evident that in the previous studies researchers mainly focused on the partial miscibility between PLA and polyester or polyether segment of TPU. There

is no work represented in the literature that investigates the compatibilization of PLA and TPU with reactive compatibilizers. It is expected that diisocyanates can be useful for reactive processing of PLA/TPU blends due to the potential interactions of diisocyanates with —OH/—COOH end groups of PLA and —OH end group of TPU under heat and shear stress during melt processing.³³ The aim of this study is to investigate the effects of PLA to TPU ratio and diisocyanate content on the compatibility and the performance of PLA/TPU blends. The mechanical, thermal, and rheological properties of the blends having the diisocyanate are determined. To have insight on the reactively compatibilized structure of PLA/TPU, the phase morphologies are investigated by means of scanning electron microscopy (SEM).

EXPERIMENTAL

Materials

PLA (trade name: PLI 005, injection molding grade) was obtained from NaturePlast (France). According to the information supplied by the manufacturer, it has a density and MFI value of 1.25 g/cm³ and 10–30 g/10 min (190°C/2.16 kg), respectively. The caprolactone diol based commercial TPUs having three different Shore A hardness values were kindly obtained from Lubrizol. These polyurethanes were abbreviated as TPU1 (75 Shore A), TPU2 (84 Shore A), and TPU 3 (90 Shore A) according to their hardness. 1,4-phenylene diisocyanate (PDI) was purchased from Sigma Aldrich company. Its melting point is 96°C and boiling point is 260°C.

Processing

Before compounding, both PLA and TPU were dried in a vacuum oven at 65°C, –4 bars for 24 hr. The compounding was done in a 15 mL twin-screw conical laboratory scale compounder (DSM Xplore Microcompounder, The Netherlands). The screw speed was fixed at 100 rpm and the barrel temperature was fixed at 200°C. The residence time during the compounding was 3 min. In order to prevent thermo-oxidative degradation of PLA, the barrel was continuously purged with Argon. At the end of compounding period, the melt was directly transferred to the DSM Xplore 12 mL laboratory injection-molding machine using the preheated transfer cylinder to obtain the standard test bars of ISO 527 5a. The melt and mold temperatures were set to 200°C and 30°C, respectively. The injection pressure was 10 bars.

The ratio of PLA/TPU in the blends were 95/5%, 80/20%, and 50/50% by weight. The amount of PDI was 0%, 0.5%, 1%, and 3% PDI by weight in the blends. The blends were labeled as shown in Figure 1.

Characterization

A universal tester (LRX PLUS, Lloyd Instrument) was used to analyze tensile behavior of the blends. The load cell used was 5 kN and the crosshead speed for the measurements was fixed at 10 mm/min. Measurements were performed, at room temperature, on dog-bone shaped tensile bars having dimensions according to ISO 527 standard.

Dynamic mechanical analysis (DMA) was performed using Metravib 01dB DMA50 instrument. Pure PLA, pure TPU2, and

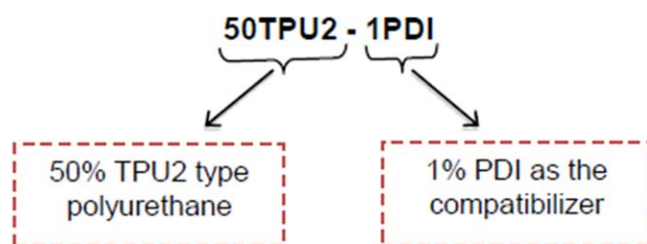


Figure 1. Explanation of the sample abbreviations. [Color figure can be viewed in the online issue, which is available at wileyonlinelibrary.com.]

the blends were investigated under uniaxial tension mode, between -60°C and 150°C , at the heating rate of $1^{\circ}\text{C}/\text{min}$ at a fixed frequency of 1 Hz. The $30 \times 4 \times 2 \text{ mm}^3$ samples were prepared by injection molding according to the method described above.

Differential scanning calorimeter (DSC) analysis was performed using Mettler Toledo DSC1 Star System in the nitrogen atmosphere. The samples for DSC analysis were cut from the narrow section of injection molded tensile bars. The analysis was conducted as follows: first samples were heated from room temperature to 200°C at the heating rate of $10^{\circ}\text{C}/\text{min}$, kept at 200°C for 3 min to erase the thermal history. Then samples were cooled to -90°C with a cooling rate of $10^{\circ}\text{C}/\text{min}$ and heated to 200°C with a heating rate of $10^{\circ}\text{C}/\text{min}$. The reported DSC results were taken from the second heating run.

The barrel of the micro-compounder was positioned on a lever, where the barrel was allowed to swivel around a stationary axis, and was counter balanced by a load-cell at the other end. The load-cell used for measuring the force was 10 kN. The measured force was the vertical force exerted by the barrel opposing the pushing forces imposed by the screws toward the bottom, while the polymer melt was pumped through the recirculation channel or die. For a given polymer, when the screw speed and the barrel temperature were fixed, the vertical force measured by the load cell represented the melt viscosity of the polymer. The detailed schematic picture of the vertical force measurement is given elsewhere.³⁴ In this study, the vertical force measurement is conducted for comparison of the melt viscosity of the materials processed at different compositions. The vertical force data were recorded at the interval of 1 min, after filling of the barrel.

The linear rheological tests were performed on a rotational rheometer (TA Ares-G2) with parallel plate geometry of 25 mm in diameter. The samples for rheological measurements were obtained by injection molding (thickness $\approx 2 \text{ mm}$) according to the method described in processing part. The stability of samples was checked through the dynamic time sweep test at 1 Hz and 200°C with the strain amplitude of 1%. All tests were performed in the linear viscoelastic region (small strain amplitude of 1%), at the constant temperature (200°C), frequency sweep in the range of $0.1\text{--}100 \text{ rad s}^{-1}$.

Phase morphologies of blends were investigated by means of SEM (JEOL JSM-6335F). The samples for SEM were cryogenically fractured in liquid nitrogen and sputter coated with gold and palladium prior to analysis.

RESULTS AND DISCUSSION

Possible Compatibilization Reactions

The interfacial reaction of PDI with PLA and TPU is shown in Figure 2. To chemically modify polyester-based polymers, chain extenders, such as diepoxides, diisocyanates, dianhydrides, bis-oxazolines, and carboimides can be used.³⁵ In this study, PDI is used to compatibilize the PLA/TPU blend systems at different compositions. It was mentioned in the literature that diisocyanates preferentially react with hydroxyl (fast reaction) [Figure 2(a)] to produce urethane, and relatively less preferentially with carboxyl to produce amide groups [Figure 2(b)].^{35,36} These type of extension reactions can form both extended PLA or TPU, which can increase the molecular weight of the individual components, and can also form the PLA-g-TPU block copolymers that play the *in-situ* compatibilizer role during compounding [Figure 2(a), 1]. In addition, there are secondary reactions taking place between diisocyanate and labile hydrogens of urethane or amide to form allophanate [Figure 2(a), 2] or urea [Figure 2(b), 5], as respectively.^{35,36} These second less favorable reactions can lead the increase in molecular weight and formation of branched or crosslinked structures, since average functionality is greater than 2. A similar reaction between PET and a diisocyanate has been shown elsewhere.³⁶ One should note that the reaction of $-\text{OH}$ groups with isocyanates is much faster than the reaction of urethane functionality with isocyanate. Therefore, it is unlikely that significant amounts of

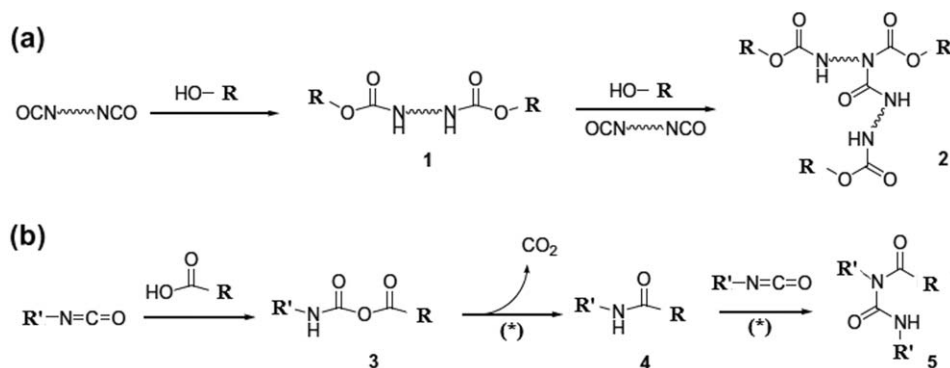
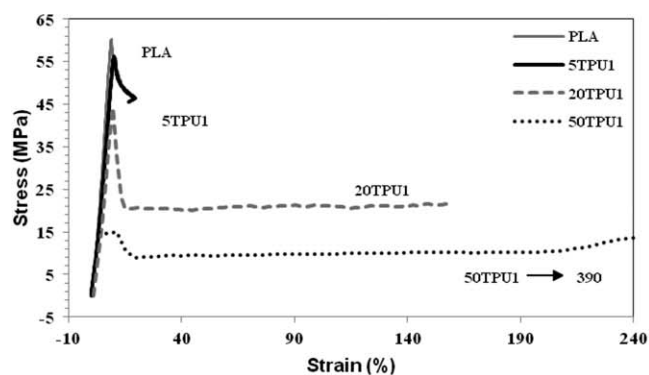
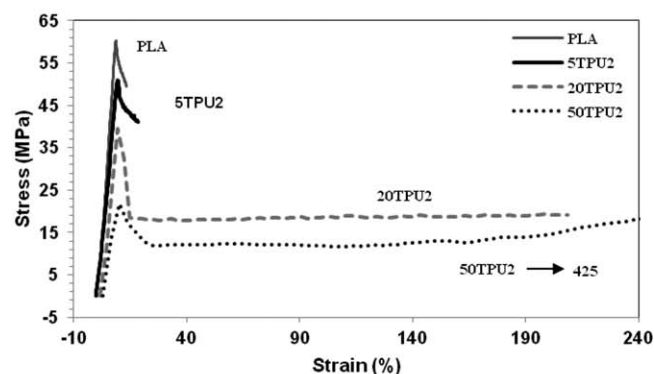


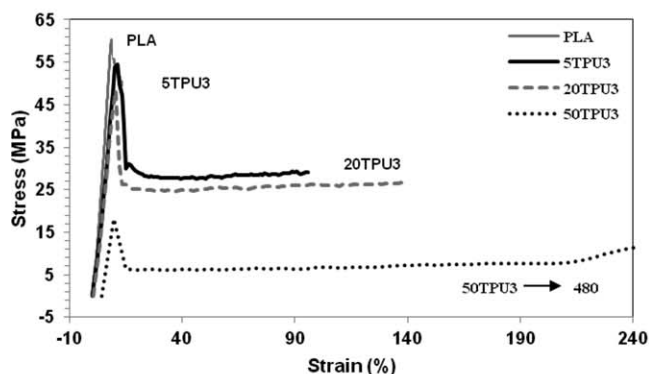
Figure 2. Chain extension and secondary branching reactions of isocyanate with PLA and/or TPU: (a) reactions of $-\text{OH}$ end groups (R: TPU or PLA); (b) reactions of $-\text{COOH}$ end groups (R: PLA and R': any alkyl group of diisocyanate). (*) the reaction with $-\text{COOH}$ end groups affords unstable *O*-acylcarbamates [3 in Figure 2(b)] that eventually decompose to amides with loss of CO_2 .



(a)



(b)



(c)

Figure 3. Stress–strain curves of PLA/TPU blends with respect to TPU type and PLA/TPU ratio: (a) TPU1, (b) TPU2, and (c) TPU3.

allophanate will be generated. In other words, the formation of branching and also crosslinking is preferentially less probable.

In order to qualitatively observe the formation of any crosslinked structure (gel), the solutions of neat polymers and compatibilized and incompatibilized blends were dissolved in THF (1 g polymer/40 mL solvent), a good solvent for both PLA and TPU types. It was observed that all blends were totally soluble in THF, therefore, it was understood that the blends were not crosslinked.

Tensile Behavior of the PLA/TPU Blends

As far as tensile properties of blends are concerned, the main target is to achieve balance between stiffness and toughness.³⁷

Similar to other composite systems, the mechanical properties of the polymer blends tend to lie between the properties of the individual components. In addition to that, the blend composition and the level of compatibility play an important role in determination of the blend property. In order to observe the effect of blend ratio and the compatibilizer (PDI) content on the tensile behavior of the blends, three different PLA/TPU ratios and three different compatibilizer contents were taken as the experimental parameters. In addition, only in tensile tests, to observe the effect of TPU structure on the properties of PLA/TPU blends, three different TPU types, that is, TPU1, TPU2, and TPU3, having different hardness values (different hard to soft segment ratio) are investigated.

Figure 3 shows the stress–strain behavior of neat PLA and incompatibilized blends having different types of TPU. Neat PLA exhibits yielding and subsequent brittle failure without any cold-drawing but, PLA/TPU blends exhibits a typical ductile characteristic such as necking and subsequent stress whitening followed by a cold-drawing zone.³⁸ The work to failure value, which is the absorbed energy in Joules (J) during the tensile testing increases in the presence of the TPU and its concentration.²⁴

The variation in tensile strength and % strain at break of the incompatibilized blends with respect to TPU types is given in Figure 4. As a general trend, the tensile strength decreases with the increasing TPU content, which is in line with the literature that focuses on the rubber toughening of PLA.^{39,40} This behavior can be attributed to both (a) weakening of the intramolecular interactions between PLA chains in the presence of TPU molecules that result in premature failure during tensile testing, and (b) the lower intrinsic tensile strength of TPUs due to their elastomeric nature. Among them, PLA/TPU3 blends exhibit slightly higher tensile strength values at any given composition. It is seen that the strain at break of the blends dramatically increases with the TPU content in comparison to the pristine PLA. These findings are in agreement with the earlier studies.⁴¹

The effect of the compatibilizer composition, TPU type, and the PLA/TPU ratio on the tensile strength and strain at break are represented in Figure 5(a,b). It is evident from the results of 20 wt % TPU containing blends [Figure 5(a)] that the tensile

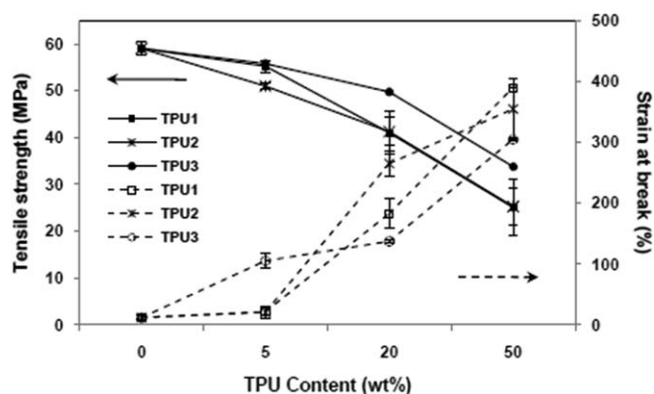


Figure 4. Tensile strength and strain at break (%) values of incompatibilized PLA/TPU blends with respect to TPU content and types.

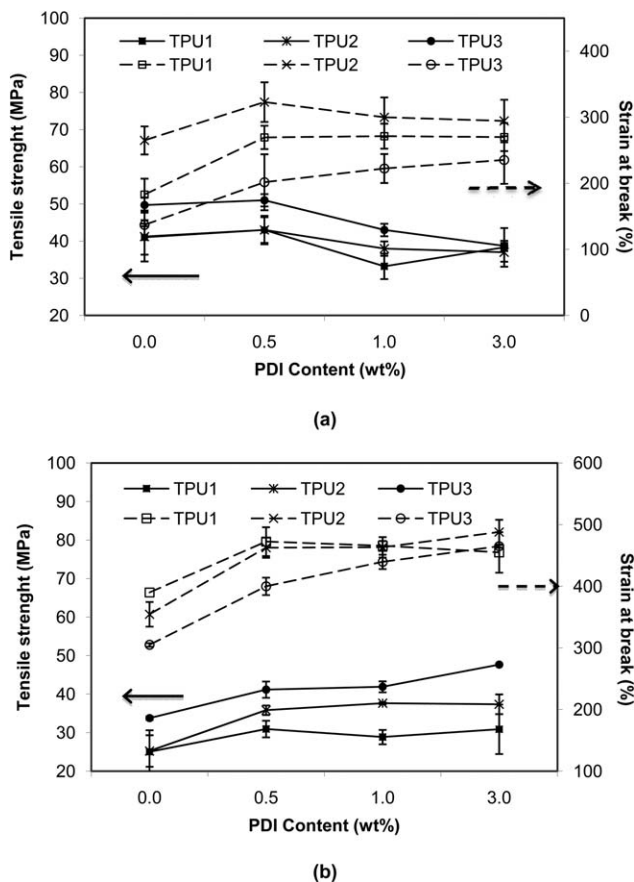


Figure 5. Tensile strength and strain at break (%) values of compatibilized blends with respect to the PDI content: (a) 20 wt % TPU and (b) 50 wt % TPU.

strength increases slightly with the addition of 0.5 wt % PDI. However, at the higher wt % of PDI (1 and 3 wt %), the effect of PDI diminishes independent of the TPU type. Similarly, the strain at break of the blends increases with the addition of 0.5 wt % PDI, but the further addition either did not make any significant change or decreases the strain at break values. The increase in tensile properties can be ascribed by the improved interfacial adhesion^{42–44} of the two phases owing to the possible H-bonding or covalent interactions given in Figure 2 in the presence of PDI. The decrease in tensile properties above 0.5 wt % loading of PDI can be explained as follows: at the lower concentration of PDI (0.5 wt %), below a saturation level of the compatibilizer, the bonded molecules are located in the interfacial area between the dispersed phase and matrix. When the saturation level of PDI is increased (above 1 wt %), the compatibilizer forms a weak boundary between the phases resulting in low strength values.⁴⁵ From the results of 50 wt % TPU containing blends [Figure 5(b)] it can be stated that the tensile strength increases considerably with the addition of 0.5 wt % PDI only, and increases slightly with the further increase in PDI (1 and 3 wt % of PDI) independent of the TPU type. These results conclusively demonstrate that due to the higher interfacial area in 50 wt % TPU containing blends, the saturation level of the compatibilizer does not exceed up to 3 wt % PDI. The TPU3 blends yield the highest tensile strength

and the lowest elongation at break value. Since TPU3 is the hardest TPU, its intrinsic tensile strength is the highest compared with the others. Therefore, the presence of PDI contributes more in the TPU3 blends strength. A similar explanation can be also given for changes in strain at break with the TPU type.

Dynamic Mechanical Properties of PLA/TPU Blends

Dynamic mechanical properties of PLA/TPU2 base blends, having different PDI ratio and TPU2 content are represented in Figure 6(a,b). Neat PLA and neat TPU2 exhibit a single transition peak at 62°C and -28°C, respectively. The PLA/TPU blends exhibit both the transitions of PLA (ca., 60°C) and TPU2 (ca., -30°C) exhibited in the enlarged plot in Figure 6(a) phases indicating a phase-separated blend system. In this case, two detectable peaks that belong to the transition temperatures (i.e., T_g) of PLA-rich and TPU-rich phases are observed in the DMA plots. However, in the presence of PDI the fact that the two T_g s shift between the T_g s of the neat polymers suggest that though the two polymers are not completely miscible, there existed an interaction between the molecules of TPU2 and PLA. This shift in T_g of the two phases is very significant in the compatibilized blends, suggesting that the presence of PDI improves

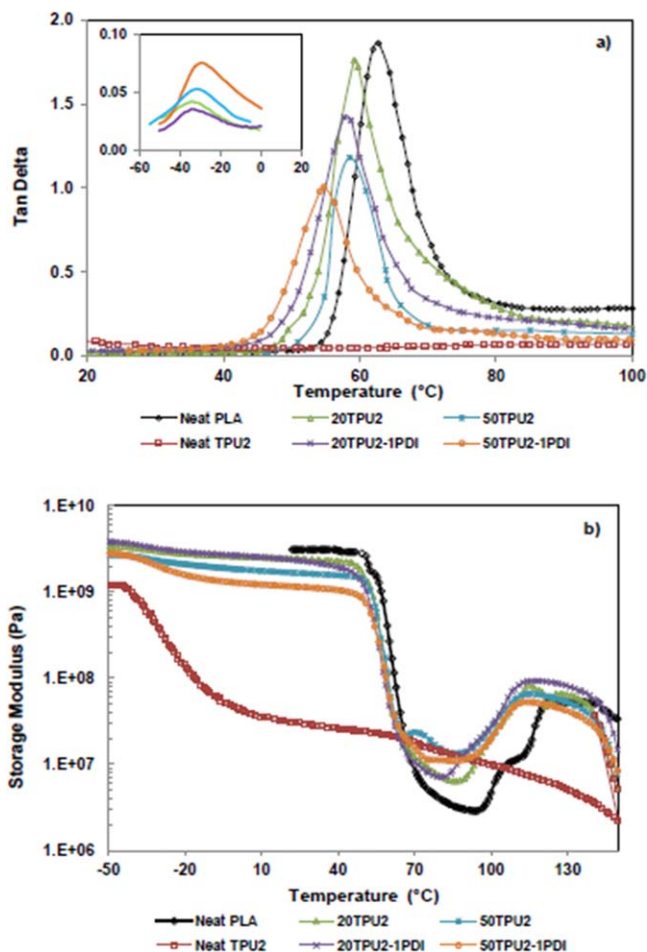


Figure 6. DMA results of PLA/TPU2 blends: (a) tan- δ , and (b) storage modulus as a function of temperature. [Color figure can be viewed in the online issue, which is available at wileyonlinelibrary.com.]

Table I. Thermal Properties of PLA, TPU2, and PLA/TPU2 Blends Obtained From DSC Heating Thermograms

Material	PLA phase			TPU phase	
	T_g (°C)	T_c (°C)	T_m (°C)	T_g (°C)	T_m (°C)
PLA	59.7	123.6	150.7	—	—
TPU2	—	—	—	-40.2	176.6
20TPU2	60.6	104.9	150.3	—	172.4
20TPU2-0.5PDI	56.0	111.9	148.1	—	—
20TPU2-1PDI	57.5	111.8	148.7	—	—
20TPU2-3PDI	57.1	112.2	148.2	—	—
50TPU2	59.2	105.3	150.0	—	173.9
50TPU2-0.5PDI	58.1	108.2	146.2	—	—
50TPU2-1PDI	57.0	109.8	145.9	—	—
50TPU2-3PDI	57.4	109.5	146.0	—	—

the compatibility of PLA and TPU phases through possible covalent interactions shown in Figure 2.

The amplitude of the $\tan \delta$ peak of the incompatibilized blends decreases monotonically with the addition of TPU2. The observed changes depend on the weight fraction of PLA in the blend, as expected [Figure 6(a)]. The reduction in $\tan \delta$ gets more pronounced in the case of compatibilized blends, that is, in the presence of PDI. The reduction in $\tan \delta$ is a clear indication of the weak damping behavior of TPU2 in the temperature range of the main relaxation of the PLA. The damping behavior becomes more dominant, due to the improved interaction between PLA and TPU2, in the presence of PDI.⁴⁶

The change in the storage modulus of neat PLA, neat TPU2, and their blends, with respect to temperature are represented in Figure 6(b). Neat PLA exhibits a high modulus below its T_g followed by a drastic drop by 3 orders of magnitude in modulus around the glass transition region. The increase in modulus around 120°C–130°C is attributed to the cold crystallization of PLA.^{31,47} Neat TPU2 exhibits typical viscoelastic behavior of an elastomeric material: a high modulus below its T_g followed by a sharp drop by 1.5 order of magnitude around the glass transition zone and an extended rubbery plateau. The storage moduli for the blends lie between the neat PLA and the neat TPU2. The blends exhibit relaxations resulting from the transitions of PLA and TPU2 phases. The increase in modulus due to the cold crystallization of PLA phase is also observed in the blends. The modulus of the blends decreases with the addition of TPU2 due to the lower intrinsic modulus of TPU2 in comparison to the neat-PLA. The storage moduli curves for 20TPU2-0PDI and 20TPU2-1PDI show strong similarities, independent of the amount of PDI.

Thermal Properties of PLA/TPU Blends

Thermal properties of the blends are investigated by means of DSC (Table I). The neat PLA can be characterized with a T_g of 59.7°C, a cold crystallization temperature (T_c) of 123.6°C and a melting temperature of (T_m) 150.7°C. Thermoplastic polyurethane, TPU2, has a T_g of -40.2°C specific to the soft segment and a T_m of 176.6°C arising from the hard segment.

Compatibility of polymer blends can be judged by observing shift in the T_g of the phases in comparison to their original values. It should be noted that the T_g of TPU phase could not be observed in the blends. In the case of incompatibilized blends, T_g of the PLA phase in the 20TPU2 and 50TPU2 blends did not show any significant change in DSC, unlike the DMA analysis. The incorporation of PDI to the PLA/TPU blends resulted in a 2°C–4°C decrease in the T_g of PLA independent of the PLA/TPU ratio. The decrease in the glass transition temperature of PLA phase in the blends suggests improved compatibility with TPU2. This result is in accordance with DMA. It should be noted that the difference between the numerical values of the T_g in DSC and DMA is arising from the frequency factor of DMA.⁴⁸

On comparing the T_c of neat-PLA and the blends, it becomes apparent that the T_c of the PLA phase in the blends shifted to lower temperatures. This can be due to the nucleation activity of TPU phase regardless of the blend composition and compatibilization. In particular, the addition of PDI results in an increase in the T_c of blends in comparison to incompatibilized ones. This can be explained by (a) the increasing polydispersity of both extended PLA and TPU, and the formation of TPU-g-PLA, and (b) possible branching in the presence of PDI. These more disordered states can be responsible from the retardation or hindrance of both the nucleation and cold-crystallization process of PLA.³⁶ The variation in PDI content from 0.5 to 3 wt % does not have a significant effect in the T_c of the compatibilized blends.

The T_m of PLA phase in the blends is not affected by blending with either 20TPU2 or 50TPU2 in the absence of PDI. In the presence of PDI (i.e., compatibilizer), T_m of the PLA phase is significantly decreased by 2°C–4°C depending on the PLA/TPU ratio. This depression in T_m may be associated with the formation of extended PLA and TPU, in other words increased polydispersity, and the formation of branching.^{49–53}

Rheology of PLA/TPU Blends

Figure 7 shows changes in the vertical force during processing. To recall, the barrel of the micro-compounder used in

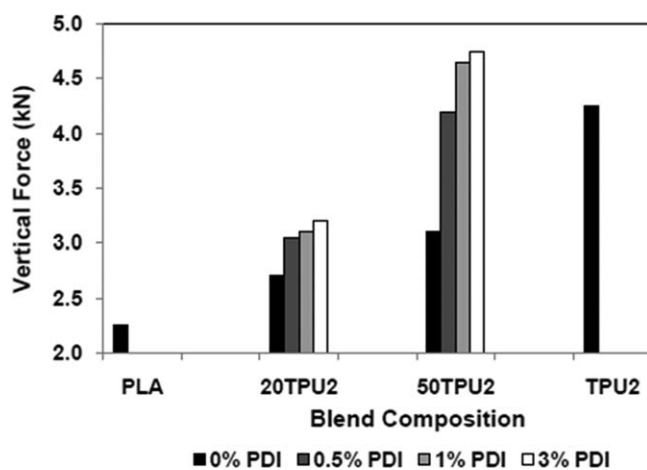


Figure 7. Vertical force values of PLA/TPU2 blends during compounding.

processing is positioned on a lever, which swivels around a stationary axis and counter balanced by a load-cell at the other end. The 10 kN load-cell measures the axial force exerted by the barrel opposing the pushing forces imposed by the screws toward the bottom while the melt is pumped through the recirculation channel or die. For a given volume of a material, when the screw speed and the barrel temperature are fixed, then the measured vertical force is proportional to the melt viscosity.³⁴ Details and schematic representation of vertical force measurement can be found elsewhere. In the current study, the vertical force measurement is conducted to verify changes in the melt viscosity of the blends as a function of matrix composition and PDI ratio. The vertical forces are obtained at 120 sec of compounding to ensure that the entire polymer is in the molten state.

Figure 7 shows changes in the vertical force with respect to the blend composition and the PDI content. From the plot it is evident that the melt viscosity at the processing conditions for the neat-PLA is the lowest. In the absence of the compatibilizer (0% PDI), the melt viscosity steadily increases with the addition

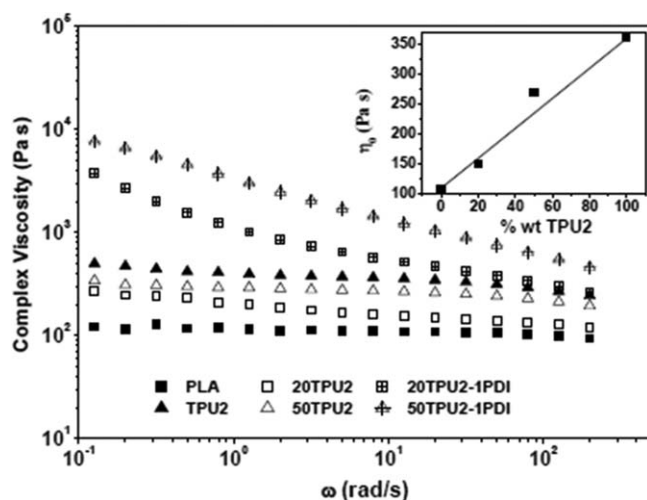


Figure 8. Dependence of complex viscosity to frequency with respect to the blend compositions. Inset shows values of zero shear viscosity for neat TPU.

of TPU. Incorporation of PDI to PLA/TPU blends increases the melt viscosity as the amount increases. This increase in the viscosity with the addition of PDI can be due to the formation of linear extended PLA, TPU, and the formation of TPU-g-PLA, a result of chain extension action of the PDI that yields branching

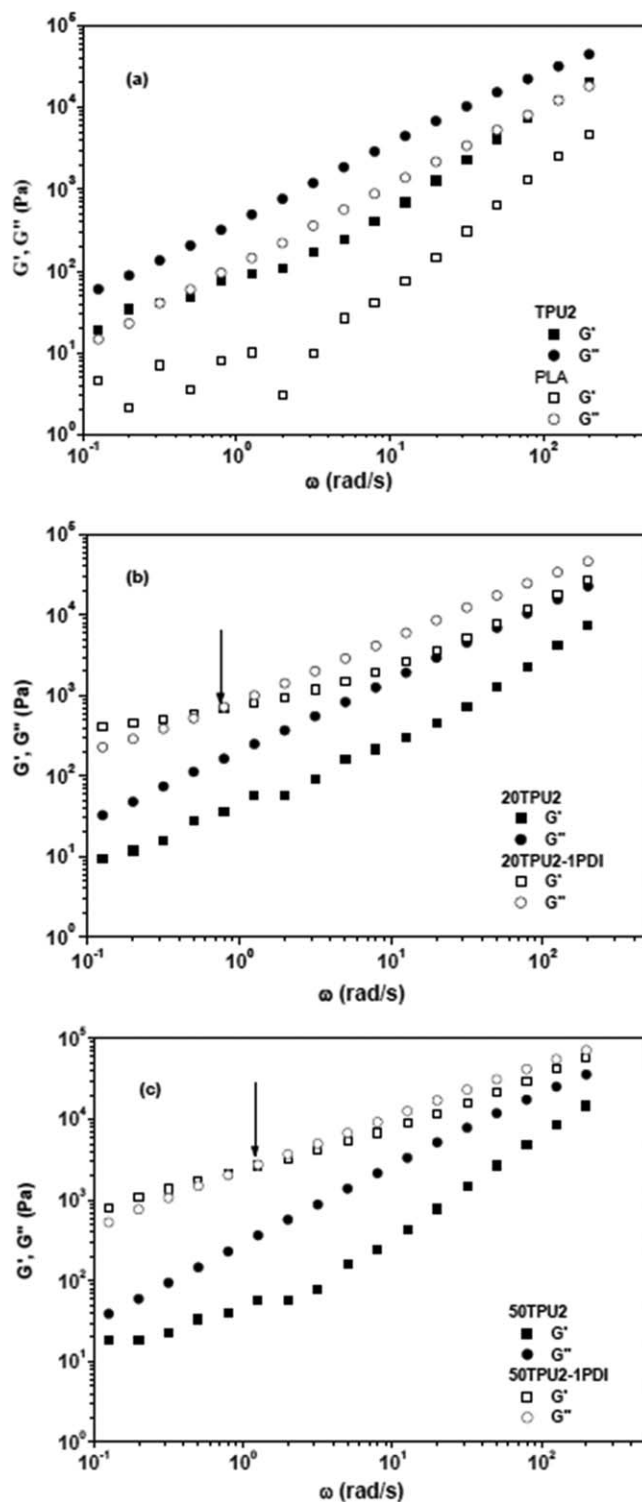


Figure 9. Dependence of storage and loss modulus to frequency: (a) Neat PLA and TPU2, (b) compatibilized and incompatibilized 20TPU2 blends, and (c) compatibilized and incompatibilized 50TPU2 blends.

and formation of higher molecular weight polymers.^{36,44} The most striking result is obtained in the 50/50 blends containing 1 and 3 wt % of PDI. In these blends, the melt viscosity is even higher than the neat-TPU, which is a proof of reactive interaction between PLA and TPU in the presence of the PDI.

Figure 8 shows the complex shear viscosity as function of frequency for neat PLA, neat TPU2, incompatibilized as well as compatibilized 20TPU2, and 50TPU2 blends. The neat PLA depicts the lowest complex viscosity. It is seen that the complex viscosities of the incompatibilized blends are in between the

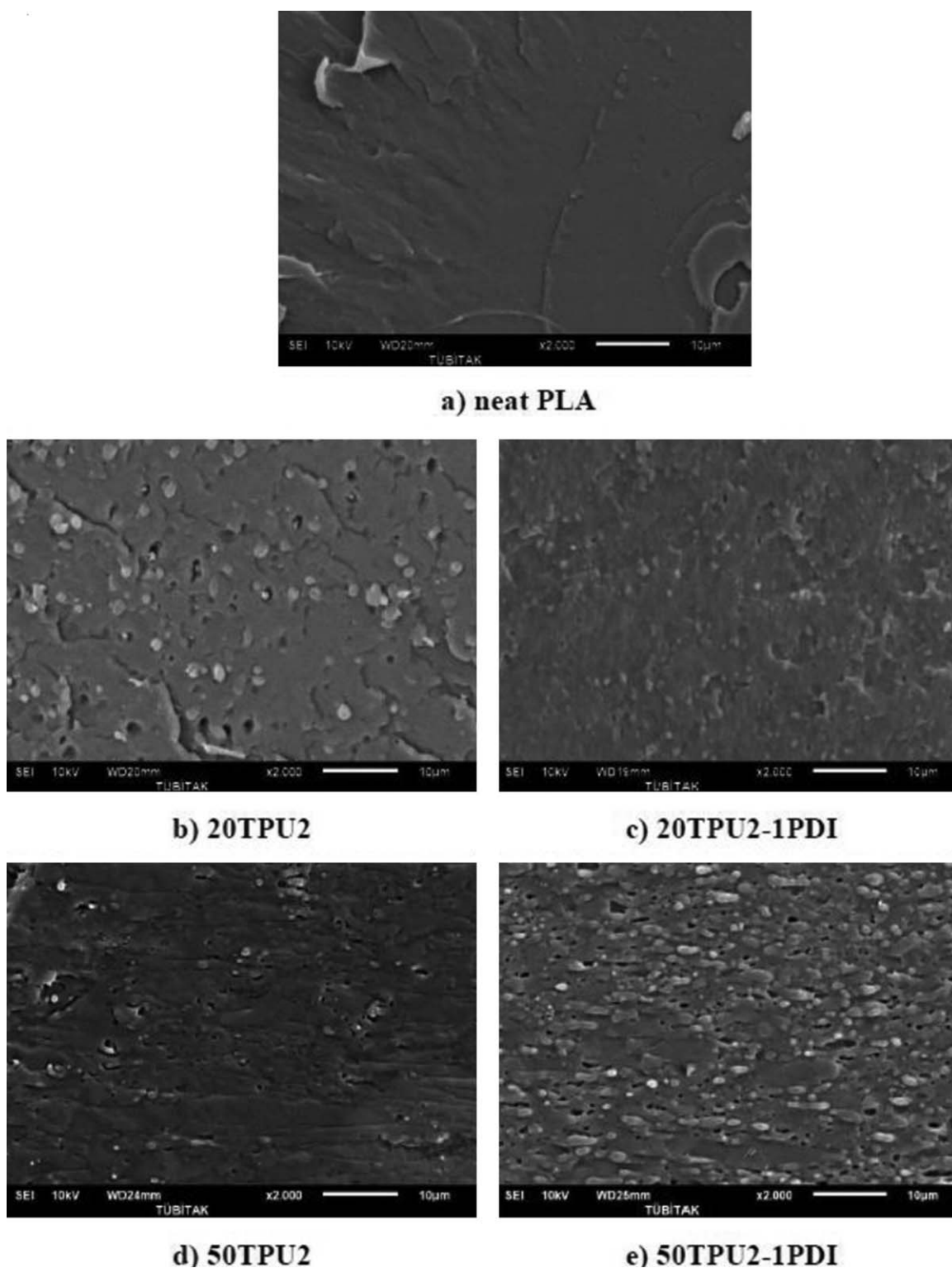


Figure 10. SEM micrographs of cryo-fractured PLA and PLA/TPU2 blends (Magnification: $\times 2000$, scale bar: 10 microns). Change in morphology becomes evident with the addition of 1 wt % of PDI in the blends of PLA and TPU2.

viscosities of the neat PLA and the TPU. The zero shear viscosity for neat polymers and incompatibilized blends are obtained from the plateau region in the low frequency range and is shown in the inset of Figure 8. The straight line represents the calculated viscosity determined from the linear mixing rule for incompatible melts.⁵⁴ The increment in zero shear viscosity with the addition of TPU, follows the mixing rule, approximately. In addition, due to shear thinning, all incompatibilized blends depict a slight decrease in the melt viscosity.⁵⁵ Incorporation of 1 wt % PDI to the incompatibilized PLA/TPU blends causes pronounced effect on both the magnitude and the frequency dependence of the complex viscosity. It is observed that the addition of PDI remarkably increases the complex viscosity of the polymer blends. A maximum increment of one order of magnitude is reached at the lowest frequencies. Additionally, shear thinning becomes more prominent in the compatibilized blends suggesting dramatic changes in the polymer blend relaxation time. This may be caused by both increment of molecular weight and possible formation of branched structures.³³

Figure 9 shows the storage (G') and loss (G'') moduli versus frequency for PLA, TPU2, incompatibilized and compatibilized 20TPU2, and 50TPU2 blends. Relaxation of neat polymers and the incompatibilized blends occurs at shorter times compared with the experimental (frequency) window in this work, thus the G'/G'' cross-over is not observed. This is in agreement with the plateau region of complex viscosities observed in most of the frequency range covered in Figure 8. In order to estimate the relaxation times for the neat polymers, the damping factor $\tan(\delta) = G''/G'$ is extrapolated to larger frequencies. The G''/G' cross-over [$\tan(\delta) = 1.0$] are estimated at frequency values of 1385 and 2319 rad/sec for TPU and PLA, respectively. Hence, relaxation of PLA melt is faster compared with TPU. As shown in Figure 9(b,c), compatibilized melts offer a different scenario compared with incompatibilized melts. With the incorporation of the PDI in the blends, G' and G'' shift to higher values independent of the blend ratio. A more dramatic effect of PDI is the appearance of a cross-over point where values of the elastic response G' becomes larger than the viscous response G'' ; turning what appears to be a terminal region at higher frequencies, into a transition-like zone at the intermediate frequencies. Thus, the relaxation process is clearly stopped, suggesting increment in molecular weight as a result of extension reactions and formation of branched structures due to the side reactions shown in Figure 2, as discussed above.^{33,56,57} These cross-over points occur at frequency values of 0.8 and 1.3 rad/sec, for the compatibilized melts having 20 and 50 wt % content of TPU, respectively. This supports the idea of the incorporation of TPU to the PLA matrix forming complex structures to recall relaxation of TPU is slower compared with PLA. As a consequence, the formation of copolymers stabilizes the interface by reducing the interfacial tension resulting in enhancement of interfacial viscosity and adhesion. This is the reason why those compatibilized blends exhibit higher G' and G'' than the incompatibilized blends. In addition, different than the incompatibilized blends, the G' and G'' curves show cross-over in the compatibilized blends (shown by an arrow) that indicate relaxation of branches formed due to the presence of PDI and increasing polydispersity index.^{33,58}

SEM of PLA/TPU Blends

In general, to achieve better performance in polymer blends, it is important to have a fine and homogeneous distribution of dispersed phase particles size. This can be obtained in the presence of a good interfacial adhesion and a reduced surface tension.^{10,59}

Figure 10 represents SEM micrographs of cryofractured surfaces of PLA and PLA/TPU2 blends. Neat PLA exhibits a homogeneous, smooth brittle fracture surface; however, both 20TPU and 50TPU blends had dual-phase morphology, where the continuous phase in the blends is PLA. The addition of PDI to the 20TPU blends results in a decrease in dispersed particle size from 1–2 microns to 0.4–1 microns on average. A similar behavior is also observed in 50TPU2 system. However, in this case dispersed phase size is found to be larger due to segregation of TPU2.⁶⁰ This confinement of phases is associated with the reduced surface tension and enhanced adhesion between the PLA and the TPU2 phases because of the possible formation of copolymers that act as compatibilizer.

CONCLUSIONS

In this study, the effect of PLA/TPU ratio and diisocyanate content on the compatibility and the performance of PLA/TPU blends are investigated. The observations are that the brittle behavior of PLA changes to ductile with the addition of TPU. The addition of 1,4 phenylene diisocyanate (PDI) in the PLA/TPU blends further improves the tensile properties of the blends and enhances the desired compatibilization of the two polymers. Tensile tests reveal that above a critical (or specific) concentration of PDI, properties of the PLA/TPU blends become independent of the PDI concentration. The presence of PDI enhances compatibilization of the PLA/TPU blend as monitored by DMA and rheological experiments. Considerable changes in the rheological response of the blends having only 1 wt % of diisocyanate are observed, for example, complex viscosity of the compatibilized blend increases and the terminal region shifts to lower frequencies. The cross-over of elastic and viscous response at relatively low frequency in the compatibilized blends indicate relaxation of branches formed due to the presence of PDI. SEM analysis further confirms that the improved compatibility between PLA/TPU occurs with the addition of PDI causing a decrease in the dispersed phase size of TPU2 in PLA.

ACKNOWLEDGMENTS

We would like to thank Lubrizol Company for providing us the TPUs. This study was granted by Kocaeli University, Turkey, with project number BAP 2011/84.

REFERENCES

1. Ho, C.-H.; Wang, C.-H.; Lin, C.-I.; Lee, Y.-D. *Polymer* **2008**, *49*, 3902.
2. Joziase, C. A. P.; Veenstra, H.; Grijpma, W.; Pennings, A. *J. Macromol. Chem. Phys.* **1996**, *197*, 2219.

3. Grijpma, D. W.; Penning, J. P.; Pennings, A. J. *Colloid Polym. Sci.* **1994**, *272*, 1068.
4. Joziassse, C. A. P.; Veenstra, H.; Topp, M. D. C.; Grijpma, D. W.; Penning, A. J. *Polymer* **1998**, *39*, 467.
5. Maa, P.; Hristova-Bogaerds, D. G.; Goossens, J. G. P.; Spoelstra, A. B.; Zhang, Y.; Lemstra, P. J. *Eur. Polym. J.* **2012**, *48*, 146.
6. Lu, J.; Qiu, Z.; Yang, W. *Polymer* **2007**, *48*, 4196.
7. Ozkoc, G.; Kemaloglu, S. J. *Appl. Polym. Sci.* **2009**, *114*, 2481.
8. Takayama, T.; Todo, M. *J. Mater. Sci.* **2006**, *41*, 4989.
9. Zhang, S.; Feng, X.; Zhu, S.; Huan, Q.; Han, K.; Ma, Y.; Yu, M. *Mater. Lett.* **2013**, *98*, 238.
10. Paul, D. R.; Bucknall, C. B. *Polymer Blends*; John Wiley & Sons: New York, **2000**, p 539.
11. Shin, B. Y.; Han, D. H. *Radiat. Phys. Chem.* **2012**, *83*, 98.
12. Wootthikanokkhan, J.; Kasemwananimit, P.; Sombatsompop, N.; Kositchaiyong, A.; Ayutthaya, S. I.; Kaabuaathong, N. *J. Appl. Polym. Sci. (Special Issue: Polysaccharides)* **2012**, *126*, E389.
13. Lee, H. S.; Kim, J. D. *Polym. Compos.* **2012**, *33*, 1154.
14. Wang, Y.; Chiao, S. M.; Hung, T. F.; Yang, S. Y. *J. Appl. Polym. Sci.* **2012**, *125*, E402.
15. Takayama, T.; Todo, M.; Tsuji, H. *J. Mech. Behav. Biomed. Mater.* **2011**, *4*, 255.
16. Kumar, M.; Mohanty, S.; Nayakb, S. K.; Parvaiz, M. R. *Bioresour. Technol.* **2010**, *101*, 8406.
17. Tatai, L.; Moore, T. G.; Adhikari, R.; Malherbe, F.; Jayasekara, R.; Griffiths, I.; Gunatillake, P. A. *Biomaterials* **2007**, *28*, 5407.
18. Gorna, K.; Gogolewski, S. J. *Biomed. Mater. Res.* **2002**, *60*, 592.
19. Gunatillake, P.; Mayadunne, R.; Adhikari, R. *Biotech. Annu. Rev.* **2006**, *12*, 1387.
20. Li, Y.; Shimizu, H. *Macromol. Biosci.* **2007**, *7*, 921.
21. Gogolewski, S.; Gorna, K.; Turner, A. S. J. *Biomed. Mater. Res. Part A* **2006**, *77*, 802.
22. Santerre, J. P.; Woodhouse, K.; Laroche, G.; Labow, R. S. *Biomaterials* **2005**, *26*, 7457.
23. Hassan, M. K.; Mauritz, K. A.; Storey, R. F.; Wiggins, J. S. *J. Appl. Polym. Sci.* **2006**, *44*, 2990.
24. Han, J.-J.; Huang, H.-X. *J. Appl. Polym. Sci.* **2011**, *120*, 3217.
25. Feng, F.; Zhao, X.; Ye, L. J. *Macromol. Sci. Part B* **2011**, *50*, 1500.
26. Yuan, Y.; Ruckenstein, E. *Polym. Bull.* **1998**, *40*, 485.
27. Hong, H.; Wei, J.; Yuan, Y.; Chen, F. P.; Wang, J.; Qu, X.; Liu, C.-S. *J. Appl. Polym. Sci.* **2011**, *121*, 855.
28. Nampoothiri, K. M.; Nair, N. R.; John, R. P. *Bioresour. Technol.* **2010**, *101*, 8493.
29. Zhong, B. Z.; Siegel, P. D. *Toxicol. Sci.* **2000**, *58*, 102.
30. Krone, C. A.; Klingner, T. D. *Pediatr. Allergy Immunol.* **2005**, *16*, 368.
31. Feng, F.; Ye, L. J. *J. Appl. Polym. Sci.* **2011**, *119*, 2778.
32. Hong, H.; Wei, J.; Yuan, Y.; Chen, F. P.; Wang, J.; Qu, X.; Liu, C.-S. *J. Appl. Polym. Sci.* **2011**, *121*, 855.
33. Harada, M.; Ohya, T.; Lida, K.; Hayashi, H.; Hirano, K.; Fukuda, H. *J. Appl. Polym. Sci.* **2007**, *106*, 1813.
34. Ozkoc, G.; Bayram, G.; Quaedflieg, M. J. *J. Appl. Polym. Sci.* **2008**, *107*, 3058.
35. Torres, N.; Robin, J. J.; Boutevin, B. *J. Appl. Polym. Sci.* **2001**, *79*, 1816.
36. Raffa, P.; Coltelli, M.-B.; Savi, S.; Bianchi, S.; Castelvetro, V. *React. Funct. Polym.* **2012**, *72*, 50.
37. Balakrishnan, H.; Attaran, S. A.; Imran, M.; Hassan, A. *J. Thermoplast. Compos.* **2013**, *1*, 1.
38. Crawford, E.; Lesser, A. *J. Polymer* **2000**, *41*, 5865.
39. Jaratrotkamjorn, R.; Khaokong, C.; Tanrattanakul, V. *J. Appl. Polym. Sci.* **2012**, *124*, 5027.
40. Bitinis, N.; Verdejo, R.; Cassagnau, P.; Lopez-Manchado, M. A. *Mater. Chem. Phys.* **2011**, *129*, 823.
41. Feng, F.; Ye, L. J. *J. Appl. Polym. Sci.* **2011**, *119*, 2778.
42. Auras, R.; Lim, L.-T.; Selke, S. E. M.; Tsuji, H. *Poly(Lactic Acid) Synthesis, Structures, Properties, Processing, and Applications*; John Wiley & Sons, Inc.: New York, **2010**.
43. Wang, H.; Sun, X.; Seib, P. J. *J. Appl. Polym. Sci.* **2001**, *82*, 1761.
44. Tamura, N.; Ban, K.; Takahashi, S.; Kasemura, T.; Obuchi, S. *J. Adhes.* **2006**, *82*, 355.
45. Tang, T.; Huang, B. *Polymer* **1994**, *35*, 281.
46. Stoclet, G.; Seguela, R. *Polymer* **2011**, *52*, 1417.
47. Martin, O.; Averous, L. *Polymer* **2001**, *42*, 6237.
48. Perkin Elmer. *Dynamic Mechanical Analysis Basics: Part2 Thermoplastic Transitions and Properties*. http://www.perkinelmer.com/CMSResources/Images/444305app_thermaldynmechanalybasicspart2.pdf; **2013**.
49. Hage, E.; Ferreira, L. A. S.; Manrich, S.; Pessan, L. A. *J. Appl. Polym. Sci.* **1999**, *71*, 423.
50. Runt, J. P.; Martynowicz, S. In *Multicomponent Polymer Materials*; American Chemical Society: Washington, D.C., **1986**, *111*, p 211.
51. Gao, G.; Wang, J.; Jinghua, Y.; Yu, X.; Ma, R.; Tang, X.; Yin, Z.; Zhang, X. *J. Appl. Polym. Sci.* **1999**, *72*, 683.
52. Ju, M.-Y.; Chang, F.-C. *Polymer* **2000**, *41*, 1719.
53. Kim, B. O.; Woo, S. I. *Polym. Bull.* **1998**, *41*, 707.
54. Grizzuti, N.; Buonocore, G.; Iorio, G. *J. Rheol.* **2000**, *44*, 149.
55. Nichetti, D.; Manas-Zloczower, I. *J. Rheol.* **1998**, *42*, 951.
56. Arsad, A.; Rahmat, A. R.; Hassan, A.; Iskandar, S. N. *J. Appl. Sci.* **2011**, *11*, 2313.
57. Shi, D.; Zhou, K.; Yang, J.; Gao, Y.; Wu, J.; Yin, J. *Macromolecules* **2002**, *35*, 8005.
58. Menges, M.; Schmidt-Naake, G. *Polymer* **1999**, *40*, 1271.
59. Liang, J. Z.; Li, R. K. Y. *J. Appl. Polym. Sci.* **2000**, *77*, 409.
60. Majumdar, M.; Paul, D. R.; Oshinski, A. *J. Polymer* **1996**, *38*, 1787.